International Journal of Heat and Technology
Vol. 36, No. 1, March, 2018, pp. 207-214
Journal homepage: http://iieta.org/Journals/IJHT

Effects of dual stratification on non-orthogonal non-Newtonian fluid flow and heat transfer

Ganganapalli Sarojamma[1*], Kata Sreelakshmi[1], Kuppalapalle Vajravelu[2]

[1] Department of Applied Mathematics, Sri Padmavati Mahila Visvavidyalayam, Tirupati 517502, India
[2] Department of Mathematics, University of Central Florida, Orlando, FL 32816, USA

Corresponding Author Email: gsarojamma@gmail.com

https://doi.org/10.18280/ijht.360128

Received: 13 October 2017
Accepted: 3 January 2018

Keywords:
non-orthogonal flow, casson fluid, stagnation point, stratification, thermal radiation.

ABSTRACT

The present analysis investigates non-orthogonal stagnation point flow and heat transfer of a dual stratified Casson fluid in the presence of radiation. A set of partial differential equations of the physical model is transformed into a system of coupled non-linear ordinary differential equations as a first step (or initially) and then are solved numerically. Effects of the physical parameters on velocity and temperature fields, and species concentration are presented through graphs. The coefficient of surface drag, local heat and mass fluxes are also presented and discussed. Authenticity of the present study is ensured by comparing our results with the available results in the literature and is found to be in a very good agreement. Undershoot of temperature (concentration) is noticed due to excessive thermal (solutal) stratification. For higher Prandtl (Schmidt's) numbers this undershoot is more significant. Stream contours are plotted for several sets of values of the stagnation point flow parameter B. Stream contours are seen to skew to the right of the stagnation point for B<0 and to the left when B>0.

1. INTRODUCTION

The study of non-Newtonian fluids with specific physical and geometrical conditions is of utmost interest and these fluids are often encountered in industrial processes. The flow characteristics cannot be easily understood due to their non-Newtonian nature. Different types of non-Newtonian fluids widely used are viscoelastic, power law, micropolar, couple stress, Casson and several others. The Casson fluid model is widely used in industry to describe paints, lubricants. The other examples include human blood, concentrated fruit juice, honey etc. Casson [1] first proposed this model to describe the flow curves of pigment oil suspensions of printing ink. Eldabe and Salwa [2] examined the heat transfer and flow characteristics of the Casson fluid between two rotating cylinders. Mustafa et al. [3] studied the boundary layer flow and heat transfer of a Casson fluid over a moving surface with parallel free stream. Several problems on Casson fluid flow in different physical situations have been studied [4-10].

Stratification refers to the formation of layers that arise due to concentration differences, temperature variations, or the presence of fluids with different densities. Double stratification occurs when both heat and mass transfer mechanisms take place simultaneously. Study of heat transfer in a doubly stratified medium has pragmatic applications in engineering. For example, heat rejection into environment like, reservoirs, lakes, rivers and oceans; thermal energy storage units which include solar pond and condensers of power plants. Yang et al. [11] treated the natural convection heat transfer from a non-isothermal vertical plate embedded in a thermally stratified medium. Jaluria and Gebhart [12] discussed the experimental and theoretical investigation to determine the effect of a stable ambient temperature stratification on the buoyancy induced flow past a vertical surface. Effects of thermal stratification on Newtonian fluid flows under different situations have been studied [13-17]. Murthy et al. [18] examined the double stratification effect on the free convective flow in a Darcy porous medium. Lakshmi Narayana and Murthy [19] extended this study to explore Soret and Dufour effects. Even though influence of double stratification of the medium on the processes of heat rejection into fluids is significant, not much work has been done in non-Newtonian fluids. Effect of thermal and solutal stratification on free convective micropolar fluid flow is investigated by Srinivasacharya and Upendar [20]. Hayat et al. [21] analyzed the slip effects on the dual stratified stagnation point flow of a chemically reactive Casson fluid on a stretching cylindrical surface. Rehman et al. [22] discussed the double stratified mixed convective flow of a Casson fluid on an inclined stretching cylinder.

Stagnation-point flows have been investigated extensively by several researches in view of their engineering and technological applications. These applications include rapid spray cooling and quenching in metal foundries, emergency core cooling systems, and glass blowing, etc. Also, analysis of stagnation point flow is of importance in estimating the frictional drag as well as rate of heat/mass transfer in the stagnation region of high speed bodies, and in the devise of thrust bearings and radial diffusers. The fluid may impinge vertically or obliquely on to the surface. Labropulu et al. [23] made the heat transfer analysis in the stagnated flow of a non-Newtonian visco-elastic fluid impinging obliquely on to the stretching sheet. Mehmood et al. [24] evaluated the flow characteristics of a non-orthogonal stagnation point flow of a Jeffrey fluid on a stretching sheet with convective boundary conditions. Khan et al. [25] studied the effect of variable viscosity on the MHD non-orthogonal stagnation point flow of a water-based nanofluid on a convective stretching sheet with

radiative heat. Mustafa et al. [26] examined MHD stagnation point flow of an upper-convected Maxwell fluid interposing non-vertically on a continuously deforming surface considering non-linear radiative heat. Rana et al. [27] explored the features of Casson fluid flowing obliquely on to the stretched surface with the effects of homogeneous and heterogeneous reactions. Tabassum et al. [28] investigated the mixed convective flow of a nanofluid pouring non-vertically on to the stretched surface.

Inspired by the aforementioned investigations, in this paper we analyze the effect of dual stratification, transverse magnetic field and thermal radiation on the non-orthogonal stagnated flow of a chemically reactive Casson fluid over a linearly stretching sheet. The analysis carried out in the present study is helpful to analyze the heat and mass characteristics of several industrial fluids that occur in many practical situations. Effects of various physical parameters on the velocity and temperature fields, and on the species, concentration are discussed. Aspects of the frictional drag coefficient, local heat, and mass fluxes are included in the discussion.

2. MATHEMATICAL FORMULATION

We consider the two-fold non-orthogonal stagnated flow of a non-Newtonian Casson fluid over a stretching sheet located at *y=0* with dual stratification.

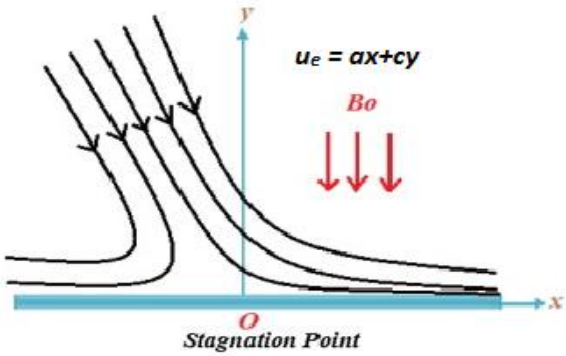

Figure 1. Physical model and coordinate system

To maintain the stretching, origin of the stretching sheet is fixed. Two equal and opposite forces are applied in opposite directions. The surface is stretched with a velocity $u_w = bx$. Let $u_e = ax + cy$ be the fluid's velocity outside the boundary layer, where *a, b* and *c* are positive constants with dimensions per time. The flow is exposed to a normal uniform magnetic field of intensity B_0 as illustrated in Figure 1.

The relevant equations for the problem are [25]:

$$\frac{\partial u}{\partial x} + \frac{\partial v}{\partial y} = 0, \tag{1}$$

$$u\frac{\partial u}{\partial x} + v\frac{\partial u}{\partial y} = \nu\left(1 + \frac{1}{\beta}\right)\frac{\partial^2 u}{\partial y^2} + u_e\frac{\partial u_e}{\partial x} - \frac{\sigma B_0^2}{\rho}(u - u_e), \tag{2}$$

$$u\frac{\partial T}{\partial x} + v\frac{\partial T}{\partial y} = \frac{k}{\rho c_p}\frac{\partial^2 T}{\partial y^2} + \frac{16\sigma^* T_\infty^3}{3k^*\rho c_p}\frac{\partial^2 T}{\partial y^2}, \tag{3}$$

$$u\frac{\partial C}{\partial x} + v\frac{\partial C}{\partial y} = D\frac{\partial^2 C}{\partial y^2} - k_0(C - C_\infty), \tag{4}$$

where, u and v are fluid velocity components along *x* and *y*-axes, respectively, ν is kinematic viscosity, $\beta = \mu_B\sqrt{2\pi_c}/P_y$ is the Casson parameter, μ_B is the plastic dynamic viscosity of the non-Newtonian fluid, P_y is the yield stress of the fluid, π_c is critical value of π based on non-Newtonian model, ρ is density of the fluid, σ is electrical conductivity, T is fluid temperature, C is fluid concentration, T_w and C_w are temperature and concentration of the surface, T_∞ and C_∞ are temperature and concentration of the ambient fluid. k is thermal conductivity of the fluid, c_p is specific heat at constant pressure, σ^* is Stefen-Boltzman constant, k^* is absorption coefficient, D is mass diffusivity and k_0 is the chemical reaction.

The appropriate boundary conditions for the problem are

$$u = u_w, v = 0, T = T_w = T_0 + m_1 x, C = C_w = C_0 + n_1 x \text{ at } y = 0, \tag{5}$$

$$u \to u_e, T \to T_\infty = T_0 + m_2 x, C \to C_\infty C_0 + n_2 x \text{ as } y \to \infty, \tag{6}$$

where m_1, m_2, n_1, n_2 are dimensional constants and T_0, C_0 are the reference temperature and reference concentration, respectively.

3. METHOD OF SOLUTION

Equations (2)-(4) can be reduced to a set of ODE's by introducing the following similarity variables

$$\eta = \sqrt{b/\nu}\, y, X = \sqrt{b/\nu}\, x. \tag{7}$$

From continuity equation (1), we can define the stream function as

$$\psi(X, \eta) = \nu[Xf(\eta) + g(\eta)], \tag{8}$$

where, $f(\eta)$ and $g(\eta)$ represent the normal and tangential components of flow respectively, such that

$$u = \sqrt{\frac{b}{\nu}}\frac{\partial \psi}{\partial \eta}, v = -\sqrt{\frac{b}{\nu}}\frac{\partial \psi}{\partial X}. \tag{9}$$

which automatically satisfy the continuity equation (1). Now, define

$$u = \sqrt{b\nu}(X f'(\eta) + g'(\eta)), v = -\sqrt{b\nu} f(\eta),$$
$$\theta(\eta) = \frac{T - T_\infty}{T_w - T_0}, \ \phi(\eta) = \frac{C - C_\infty}{C_w - C_0}. \tag{10}$$

Substituting equation (10) into (2) – (4), we obtain

$$\left(1 + \frac{1}{\beta}\right) f''' + ff'' - f'^2 - M(f' - A) + A^2 = 0, \tag{11}$$

$$\left(1 + \frac{1}{\beta}\right) g''' + fg'' - f'g' - M(g' - B\eta) + RB = 0, \tag{12}$$

$$\left(1+\frac{4}{3}Nr\right)\theta'' + Pr(f\theta' - f'\theta - \varepsilon_1 f') = 0, \quad (13)$$

$$\phi'' + Sc(f\phi' - f'\phi - \varepsilon_2 f' - \gamma\phi) = 0. \quad (14)$$

The associated boundary conditions are

$$f(0) = 0,\ f'(0) = 1, g'(0) = 0,\ \theta(0) = 1-\varepsilon_1,\ \phi(0) = 1-\varepsilon_2, \quad (15)$$

$$f'(\infty) \to A,\ g''(\infty) \to B, \theta(\infty) \to 0,\ \phi(\infty) \to 0. \quad (16)$$

From equation (16), it can be easily seen that $f(\eta) = A\,\eta + R$ as $\eta \to \infty$, where R is the boundary layer displacement constant to be determined. Let

$$g'(\eta) = B\,G(\eta)) \quad (17)$$

Substituting equation (17) into equations (12), (15) and (16), we obtain

$$\left(1+\frac{1}{\beta}\right)G'' + fG' - Gf' - M(G-\eta) + R = 0, \quad (18)$$

$$f(0) = 0,\ f'(0) = 1, G(0) = 0,\ \theta(0) = 1-\varepsilon_1,\ \phi(0) = 1-\varepsilon_2, \quad (19)$$

$$f'(\infty) \to A,\ G'(\infty) \to 1, \theta(\infty) \to 0,\ \phi(\infty) \to 0, \quad (20)$$

where, $M = \sigma B_0^2/\rho b$ is magnetic field parameter, $A = a/b$ and $B = c/b$ are free stream stagnation flow parameters, $Pr = \rho c_p \nu\,/k$ is Prandtl number, $Nr = 4\sigma^* T_\infty^3/kk^*$ is thermal radiation parameter, $Sc = \nu/D$ is Schmidt number, $\varepsilon_1 = m_2/m_1$ is thermally stratified parameter, $\varepsilon_2 = n_2/n_1$ is solutal stratified parameter and $\gamma = k_0/b$ is chemical reaction parameter.

The surface drag coefficient C_f, Nusselt number Nu at the boundary representing local heat flux Sherwood number Sh describing the local mass flux are defined by

$$C_f = \frac{\tau_w}{\rho u_e^2},\ Nu = \frac{xq_w}{k(T_w - T_\infty)},\ Sh = \frac{xm_w}{D(C_w - C_\infty)}, \quad (21)$$

where the wall shear stress τ_w, the surface heat flux q_w and mass flux m_w are given by

$$\tau_w = \mu\left(1+\frac{1}{\beta}\right)\left(\frac{\partial u}{\partial y}\right)_{y=0},\ \ q_w = -kx\left(1+\frac{16\sigma^* T^3}{3kk^*}\right)\left(\frac{\partial T}{\partial y}\right)_{y=0},\ m_w = -D\left(\frac{\partial C}{\partial y}\right)_{y=0}. \quad (22)$$

and μ is dynamic viscosity of the fluid.

Using equation (22) in equation (21), we obtain

$$C_f = \left(1+\frac{1}{\beta}\right)(Xf''(0) + BG'(0)),\ Nu = -\left(1+\frac{4}{3}Nr\right)\theta'(0),\ Sh = -\phi'(0). \quad (23)$$

The position X_f of attachment of dividing stream contour is determined by zero wall shear stress as

$$X_f = -\frac{BG'(0)}{f''(0)}.$$

The set of coupled equations (11), (18), (13) and (14) with the boundary conditions (19) and (20) are solved using RKF45 numerical scheme and is verified by comparing the values of $f''(0)$ and $G'(0)$ with those of Labropulu et al. [23], Nadeem et al. [29], Khan et al. [25] in the absence of magnetic field and for the case of a Newtonian fluid for different values of A. The data in Table 1 shows that the present results are in very good agreement.

Table 1. Comparison values of $f''(0)$ and $G'(0)$ for various values of A when $M = 0, \beta \to \infty$

A	R	Labropulu et al. [23]		Nadeem et al. [29]		Khan et al. [25]		Present Results	
		$f''(0)$	$G'(0)$	$f''(0)$	$G'(0)$	$f''(0)$	$G'(0)$	$f''(0)$	$G'(0)$
0.1	-0.791705	-0.96938	0.26278	-0.96938	0.26332	-0.969386	0.26332	-0.96938	0.26332
0.3	-0.519499	-0.84942	0.60573	-0.84942	0.60631	-0.849420	0.60631	-0.84942	0.60631
0.8	-0.114527	-0.29938	0.93430	-0.29938	0.93472	-0.299388	0.93472	-0.29938	0.93472
2.0	0.410407	2.01750	1.16489	2.01750	1.16521	2.017502	1.16521	2.01750	1.16521
3.0	0.693053	4.72928	1.23438	4.72928	1.23465	4.729282	1.23465	4.72928	1.23465

4. RESULTS AND DISCUSSION

The aim of this investigation is to analyze the impact of radiative heat transfer, dual stratification and chemical reaction on the MHD non-orthogonal Casson fluid directed towards the surface of stretching. The obtained results are presented graphically for several sets of physical parameters.

Figure 2 points out that the horizontal velocity $f'(\eta)$ decreases with increasing values of the non-Newtonian rheology parameter (β) due to increase in plastic dynamic viscosity. In the limiting case of $\beta \to \infty$, that is, when the fluid is viscous and in the absence of magnetic field (M) and when $A = 1$, equation (11) has an exact solution $f(\eta) = \eta$ which leads to $u = ax$ and $v = -ay$. In this case [30], it can be said that the velocity distribution is same as that of the inviscid flow, so that there is no boundary layer formation near the stretching surface. Figure 3 displays the development of the profiles of oblique velocity gradient $G'(\eta)$ with β. It is interesting to observe that $G'(\eta)$ increases rapidly near the boundary with steepened profiles and is an increasing function of Casson parameter in the vicinity of the boundary ($0 \le \eta \le 2.929$) and has a reversal trend in the region $2.929 \le \eta \le 8.687$.

Figure 4 suggests that the free stream stagnation flow parameter (A) has an enhancing impact on velocity. It can be

seen that the Casson fluid flow contains a specific boundary layer structure when A exceeds unity ($A > 1$) and the boundary layer thickness reduces for increasing A. This may be due to the fact that a fixed value of b, when $A > 1$ the flow corresponds to an increase in the straining motion in the neighbourhood of stagnation point leading to enhancement of acceleration of the external stream and thus the thinning of the boundary layer takes place for increasing values of A. Further, it is clear that when $A < 1$, the boundary layer pattern gets reversed owing to the fact that when $A < 1$, the velocity of the surface surmounts the stagnation velocity of the external stream. We see from Figure 5, when $A > 1$ for small values of free stream stagnation flow parameter $A = 0.5$ the oblique velocity gradient $G'(\eta)$ increases rapidly near the boundary reaching its maximum and later decreases eventually attains its free stream value. The profiles of $G'(\eta)$ are convex in nature. For $A > 1$ though a similar trend in $G'(\eta)$ is noticed the profiles are concave.

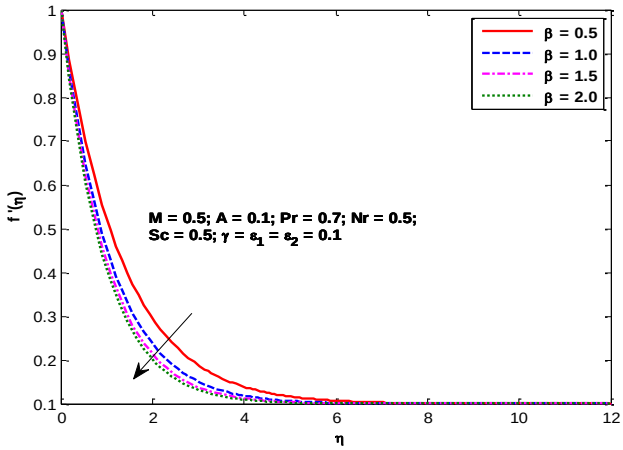

Figure 2. Variation of β on $f'(\eta)$

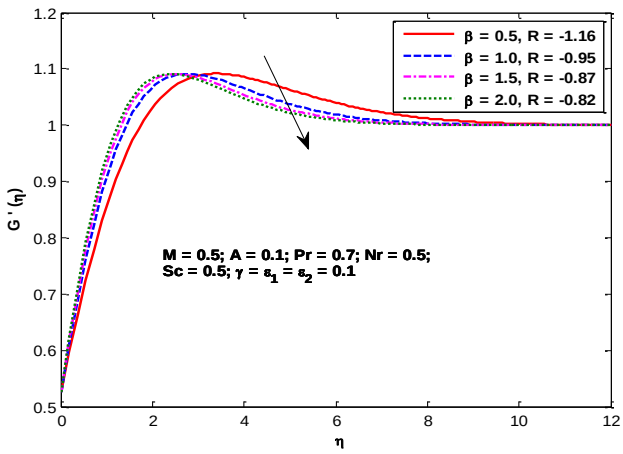

Figure 3. Variation of β on $G'(\eta)$

Figure 6 depicts the depreciation of $f'(\eta)$ for higher intensities of the magnetic field (M). This is in conformity with the fact that the stronger Lorentz force, generated as a result of higher magnetic field strength, heavily opposes the fluid motion. From Figure 7, we see that as M takes higher values the oblique velocity gradient $G'(\eta)$ increases near the wall and subsequently it reduces.

Figure 8 shows the effect of thermal stratification on temperature for $Pr = 0.7$ and $Pr = 3.0$. It is seen that temperature gradients decrease for higher Prandtl number near the surface and the temperatures are lesser than those when $Pr = 0.7$ due to smaller diffusivity. It is seen that the temperature decreases with increasing ε_1 in both cases of Pr. When $Pr = 0.7$ and $\varepsilon_1 = 0.3$, it is observed that there is a small undershoot of temperature or negative temperature away from the boundary due to excessive stratification. When $Pr = 3.0$ the undershoot is noticed even for smaller ε_1 and is more significant with increase in ε_1 due to the cumulative impact of smaller thermal diffusivity and excessive thermal stratification. Similar characteristics have been noticed in previous studies of natural convection flows [12, 31]. Physically, it may be explained that the ambient temperature T_∞ increases downstream. Hence the flow coming from below tends to have a temperature smaller than that of the local temperature resulting in undershoot of temperature. Figure 9 shows that the temperature is enhanced predominantly for larger values of the thermal radiation parameter (Nr) as thermal radiation facilitates more heat to the fluid leading to an increase in the energy transport to the fluid. Similar trend had been observed in ealier investigation in non-Newtonian fluids [32, 33]. The associated thermal boundary layers become thicker for increasing values of Nr. Increase in Nr amounts to decrease in the absorption coefficient which leads to the enhancement of temperature in the boundary layer. Increased Nr spreads the associated thermal boundary layers.

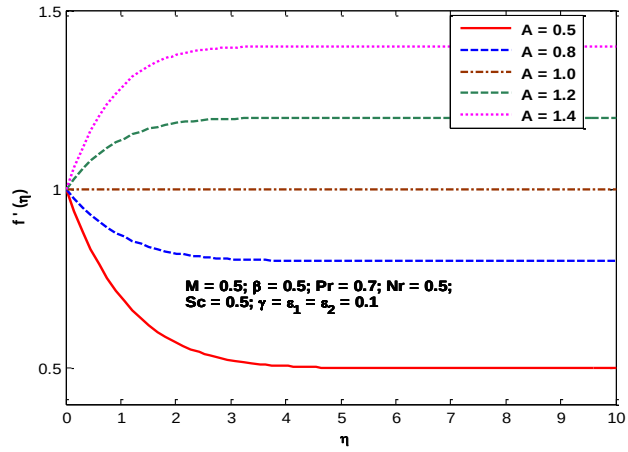

Figure 4. Variation of A on $f'(\eta)$

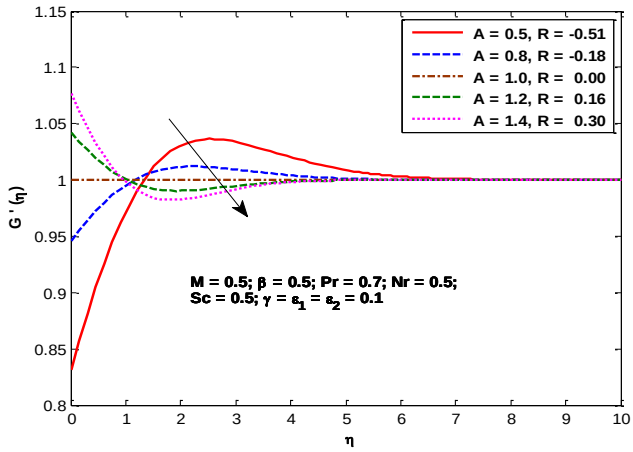

Figure 5. Variation of A on $G'(\eta)$

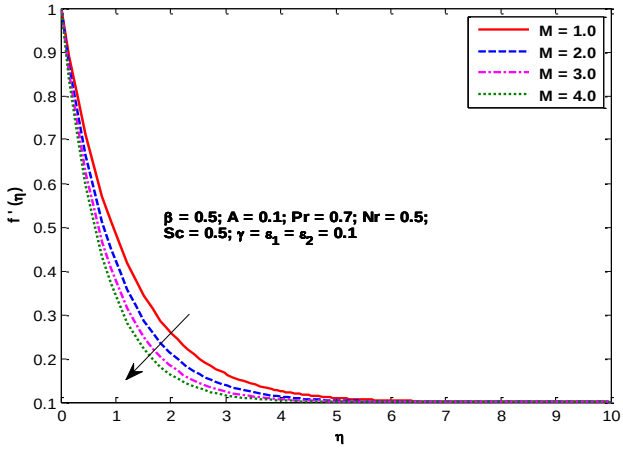

Figure 6. Variation of M on $f'(\eta)$

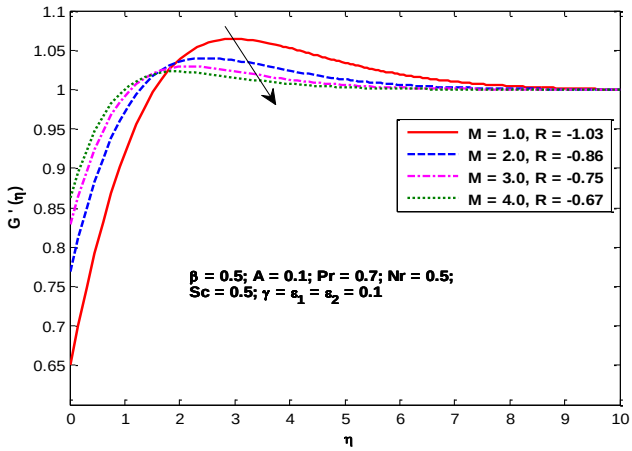

Figure 7. Variation of β on $G'(\eta)$

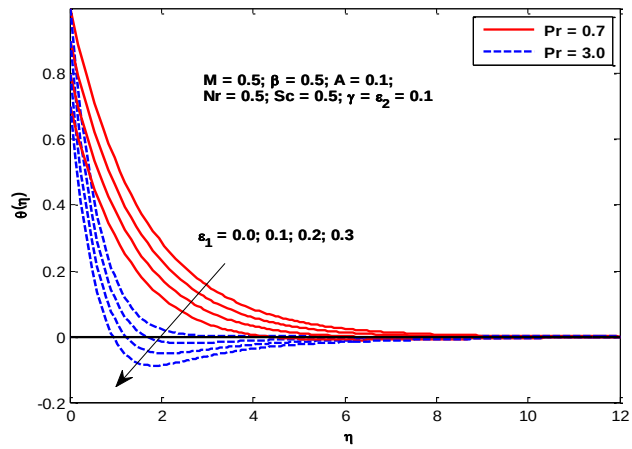

Figure 8. Variation of ε_1 and Pr on $\theta(\eta)$

Figure 10 shows the variation of solutal stratification parameter (ε_2) and Schmidt's number (Sc) on species concentration. Since the role of Prandtl number on temperature is similar to that of Schmidt's number on concentration, it can be seen that the influence of solutal stratification parameter on species concentration is exactly same as that of thermal stratification parameter on temperature distribution. Influence of chemical reaction parameter (γ) on species concentration is plotted in Figure 11. Effect of chemical reaction is to enhance the rate of interfacial mass transfer. When species concentration at the boundary is greater than that of the free stream, a gradual reduction in concentration occurs. It is observed that for a fixed value of γ, concentration of chemical species is diluted along η in the region $0 \leq \eta \leq 5$ and is seen to be a reducing function of γ. Higher values of γ result in thinning of solutal boundary layers due to weaker molecular diffusivity.

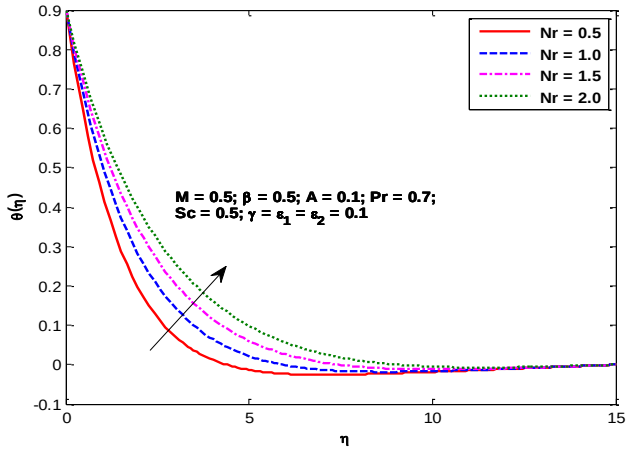

Figure 9. Variation of Nr on $\theta(\eta)$

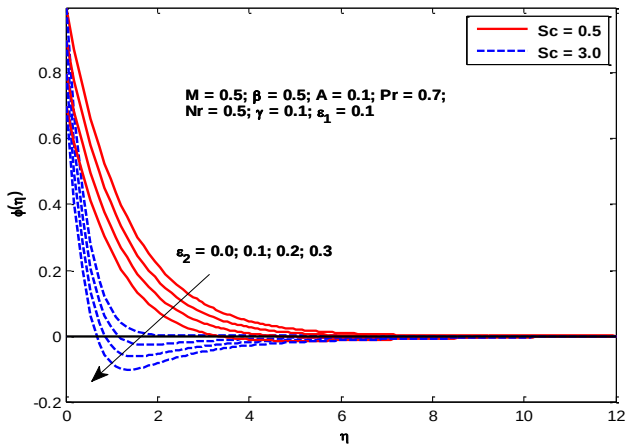

Figure 10. Variation of ε_2 and Sc on $\phi(\eta)$

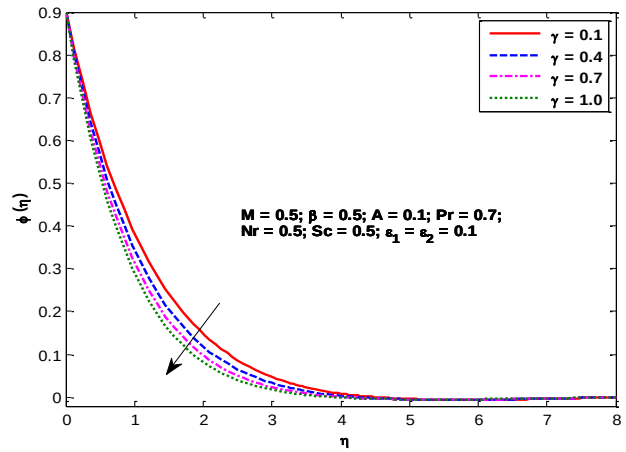

Figure 11. Variation of γ on $\phi(\eta)$

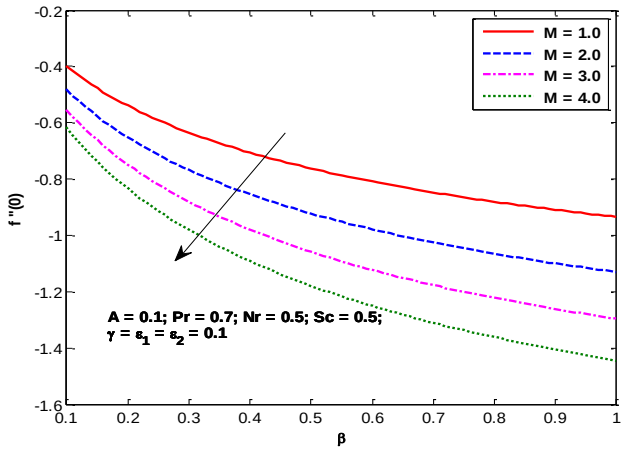

Figure 12. Variation of β and M on $f''(0)$

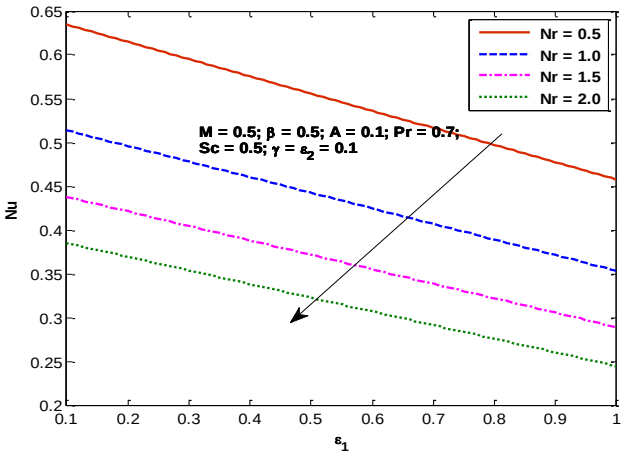

Figure 13. Variation of ε_1 and Nr on Nu

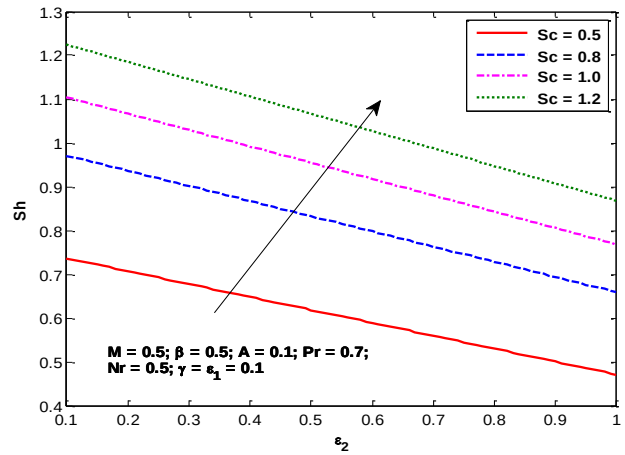

Figure 14. Variation of ε_2 and Sc on Sh

From Figure 12, it can be inferred that the combined influence of non-Newtonian rheology (β) and magnetic field (M) is to decrease the normal component of the surface drag coefficient considerably due to retardation in fluid flow. It is observed that a reduction in the surface drag coefficient when $M = 4.0, \beta = 1.0$ is almost fourfolds to that of the case when $M = 1$ and $\beta = 0.1$. From Figure 13 the local heat flux (Nu) is seen to be a decreasing function of ε_1 and Nr. When $Nr = 0.5$, as ε_1 changes from 0.1 to 1.0, the Nu reduces in the range from 0.64 to 0.38. For the same range of ε_1, when $Nr = 2.0$, the reduction in Nu is from 0.36 to 0.26. Figure 14 shows a plot of Sherwood number (Sh) versus solutal stratification number for different values of Schmidt's number. From this figure we see that Sherwood number reduces with increase in ε_2 and an opposite trend occurs with Schmidt's number. Figure 15 shows that for $B < 0$, the streamlines are skewed to the right of the stagnation point and to the left for $B > 0$ as expected. However, the streamlines are vertically oriented when $B = 0$.

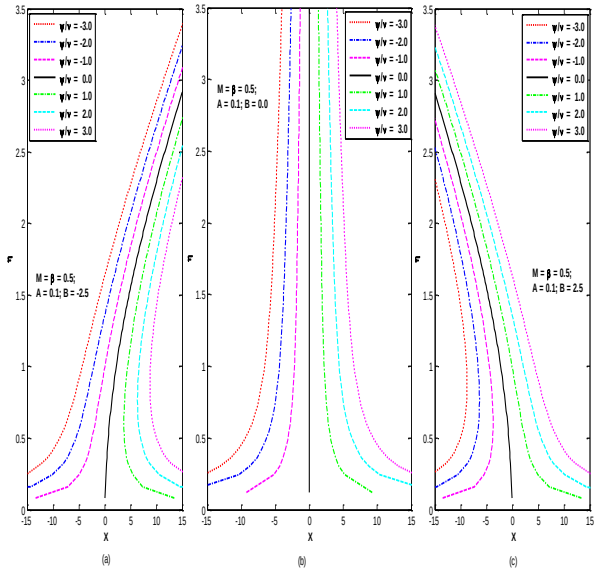

Figure 15. Streamline patterns for the oblique flow (a) non-aligned pattern for $B = -2.5$; (b) aligned pattern for $B = 0$; (c) non-aligned pattern for $B = 2.5$

5. CONCLUSIONS

Some of the interesting outcomes of the investigation are as follows:

- Cumulative effect of non-Newtonian rheology of the fluid and Lorentz force is to repress the horizontal velocity component and oblique velocity gradient considerably.
- Excessive thermal (solutal) stratification causes undershoot of temperature (species concentration).
- Non-dimensional temperature increases with increased thermal radiation parameter while thermal stratification parameter and Prandtl number have a reverse influence.
- Species concentration is diluted with increasing chemical reaction parameter and Schmidt's number.
- Normal component of the frictional drag decreases with Casson parameter and magnetic field parameter.
- Nusselt number diminishes with thermal radiation parameter and thermal stratification parameter.
- Local mass flux increases with Schmidt's number whereas solutal stratification parameter has a decreasing influence.
- Contours of the stream function are oblique to the left of the stagnation point for $B > 0$ as a result of straining motion and a reversal trend is noticed for $B < 0$.

ACKNOWELEDGEMENTS

The authors thank the anonymous reviewers and the Editor for their constructive suggestions which led to the improvement of the paper.

REFERENCES

[1] Casson N. (1959). A flow equation for pigment oil suspensions of printing ink type. In Rheology of Dispersed Systed, (Edited by C.C. Mill), Pergamon Press, Oxford 84-102.

[2] Eldabe NTM, Salwa MGE. (1995). Heat transfer of MHD non-Newtonian Casson fluid flow between two rotating cylinders. J. Phys. Soc. Japan 64: 41.

[3] Mustafa M, Hayat T, Pop I, Aziz A. (2011). Unsteady boundary layer flow of a Casson fluid due to an impulsively started flat plate. Heat Transfer – Asian Research 40: 563-576.

[4] Hayat T, Farooq M, Iqbal Z. (2013). Stretched flow of Casson fluid with variable thermal conductivity. Walailak J. Sci. & Tech 10: 181-190.

[5] Bhattacharyya K, Hayat T, Ahmed A. (2013). Analytical solution for magnetohydrodynamic boundary layer flow of Casson fluid over a stretching/shrinking sheet with wall mass transfer. Chin. Phys. B 22: 024702-1–6.

[6] Gireesha BJ, Mahanthesh B, Rashidi MM (2015). MHD boundary layer heat and mass transfer of a chemically reacting Casson fluid over a permeable stretching surface with non-uniform heat source/sink. International Journal of Industrial Mathematics 7: 247-260.

[7] Hayat T, Farooq M, Alsaedi A. (2015). Thermally stratified stagnation point flow of Casson fluid with slip conditions. International Journal of Numerical Methods for Heat and Fluid Flow 25: 724-748.

[8] Sarojamma G, Sreelakshmi K, Vasundhara B. (2016). Mathematical model of MHD unsteady flow induced by a stretching surface embedded in a rotating Casson fluid with thermal radiation. IEEE 1590-1595.

[9] Vijaya N, Sreelakshmi K, Sarojamma G. (2017). Nonlinear radiation effect on Casson fluid saturated non-Darcy porous medium International Journal of Mathematical Archive 8: 39-52.

[10] Kalyani K, Sreelakshmi K, Sarojamma G. (2017). The three-dimensional flow of a non-Newtonian fluid over a stretching flat surface through a porous medium with surface convective conditions. Global Journal of Pure and Applied Mathematics 13: 2193-2211.

[11] Yang KT, Novotny JL, Cheng YS. (1972). Laminar free convection from a non-isothermal plate immersed in a temperature stratified medium. Int. J. Heat Mass Transfer 15: 1097-1109.

[12] Jaluria Y, Gebhart B. (1974). Stability a transition of buoyancy-induced flows in a stratified medium. J. Fluid Mech. 66: 593-612.

[13] Chen CC, Eichhorn R. (1976). Natural convection from a vertical surface to stratified fluid. ASME J. Heat Trans. 98: 446-451.

[14] Kulkarni AK, Jacob HR, Hwang JJ. (1987). Similarity solution for natural convection flow over an isothermal vertical wall immersed in a thermally stratified medium. Int. J. of Heat and Mass Trans. 30: 691-698.

[15] Takhar HS, Chamkha AJ, Nath G. (2001). Natural convection flow from a continuously moving vertical surface immersed in thermally stratified medium. Heat Mass Transf. 38: 17-24.

[16] Saha SC, Hossain MA. (2004). Natural convection flow with combined buoyancy effects due to thermal and mass diffusions in a thermally stratified media, Non Linear Analysis Modell. Control 9: 89-102.

[17] Singh G, Sharma PR, Chamkha AJ. (2010). Effect of thermally stratified ambient fluid on MHD convective flow along a moving non-isothermal vertical plate. International Journal of Physical Sciences 5: 208-215.

[18] Murthy PVSN, Srinivasacharya D, Krishna PVSSSR. (2004). Effect of double stratification on free convection in Darian porous medium. ASME J. Heat Transfer 126: 297-300.

[19] Lakshmi Narayana PA, Murthy PVSN. (2006). Soret and Dufour effects on free convection heat and mass transfer in a doubly stratified Darcy porous medium. ASME J. Heat Transfer 128: 1204-1212.

[20] Srinivasacharya D, Upendar M. (2013). Effect of double stratification on MHD free convection in a micropolar fluid. J. Egyptian Math. Soc. 21: 370–378.

[21] Hayat T, Farooq M, Alsaedi A. (2015). Thermally stratified stagnation point flow of Casson fluid with slip conditions. International Journal of Numerical Methods for Heat and Fluid Flow 25: 724–748.

[22] Rehman KU, Malika AA, Malika MY, Sandeep N, Noor US. (2017). Numerical study of double stratification in Casson fluid flow in the presence of mixed convection and chemical reaction. Results in Physics 7: 2997-3006.

[23] Labropulu F, Li D, Pop I. (2010). Non-orthogonal stagnation-point flow towards a stretching surface in a non-Newtonian fluid with heat transfer. International Journal Thermal Sciences 49: 1042-1050.

[24] Mehmood R, Nadeem S, Akbar N. (2015). Oblique stagnation flow of Jeffery fluid over a stretching convective surface. Int. J. Numerical Methods for Heat & Flow 25: 454–471.

[25] Khan WA, Makinde OD, Khan ZH. (2016). Non-aligned MHD stagnation point flow of variable viscosity nanofluids past a stretching sheet with radiative heat. International Journal of Heat and Mass Transfer, 96: 525–534.

[26] Mustafa M, Mushtaq A, Hayat T, Alsaedi A. (2016). Non-aligned MHD stagnation-point flow of upper-convected Maxwell fluid with nonlinear thermal radiation. Neural Comput. & Applic. https://doi.org/10.1007/s00521-016-2761-2

[27] Rana S, Rashid M, Akbar NS. (2016). Mixed convective oblique flow of a Casson fluid with partial slip, internal heating and homogeneous–heterogeneous reactions. Journal of Molecular Liquids 222: 1010-1019.

[28] Tabassum R., Mehmood R., Akbar NS. (2017). Magnetite micropolar nanofluid non-aligned MHD flow with mixed convection. Eur. Phys. J. Plus 132: 1-15.

[29] Nadeem S, Mehmood Rd, Akbar NS. (2015). Partial slip effect on non-aligned stagnation point nanofluid over a stretching convective surface. Chin. Phys., B 24: 014702-1–8.

[30] Chiam TC. (1994). Stagnation-point flow towards a stretching plate. J. Phys. Soc. Jpn. 63: 2443–2444.

[31] Cheesewright R. (1967). Natural convection from a plane, vertical surface in non-isothermal surroundings. Int. J.

Heat Mass Transfer 10: 1847-1859.
[32] Amos OP, Ismail GB, Bakai IO. (2016). Heat and mass transfer on MHD viscoelastic fluid flow in the presence of thermal diffusion and chemical reaction. International Journal of Heat and Technology 34: 15-26.
[33] Mabood F, Ibrahim SM, Lorenzini G, Lorenzini E. (2017). Radiation effects on Williamson nanofluid flow over a heated surface with magnetohydrodynamics. International Journal of Heat and Technology 35: 196-204.